

## **Exact Results for Wetting and Filling on a Triangular Lattice<sup>1</sup>**

**D. B. Abraham,<sup>2</sup> Ville Mustonen,<sup>2-4</sup> and A. J. Wood<sup>2</sup>**

---

New exact analytical results are described for surface tension on the triangular Ising lattice. The triangular Ising lattice forms naturally  $60^\circ$  and  $120^\circ$  corners, and a thermodynamic argument is used, which incorporates the exact results, to obtain conditions for the filling transition for both angles. Monte Carlo simulations with Wang–Landau sampling are performed to independently verify the applicability of this argument. Results are in agreement with previous conjectures for the phase boundary in these systems.

---

**KEY WORDS:** filling; Monte Carlo; triangular Ising lattice; wetting.

### **1. INTRODUCTION**

The phenomenon of filling, that is, of wetting modified by grooving or pitting substrates, has been a subject of considerable recent work [1–11], motivated by both potential practical applications and by what has turned out to be an interesting new type of phase transition [12,13]. In a typical situation, the region of parameter space in which there is filling contains, and is larger than, the region of wetting. This supplements the tuning of wetting effected by chemical means [14]. The key intellectual challenge is that interfaces between coexisting phases display spatial fluctuations

---

<sup>1</sup>Paper presented at the Fifteenth Symposium on Thermophysical Properties, June 22–27, 2003, Boulder, Colorado, U.S.A.

<sup>2</sup>Department of Physics, Theoretical Physics, University of Oxford, 1 Keble Road, Oxford OX1 3NP, United Kingdom.

<sup>3</sup>Laboratory of Computational Engineering, Helsinki University of Technology, P.O. Box 9203, FIN-02015, Finland.

<sup>4</sup>To whom correspondence should be addressed. E-mail: ville.mustonen@physics.oxford.ac.uk

about their mean position which diverge with the system size. Thus, theories which neglect these or restrict them by uncontrolled approximations should be treated with considerable caution. To date, there is just one exactly solvable model starting from a molecular-level Hamiltonian [8] (the rectangular Ising ferromagnet) which displays such a filling transition. This Ising calculation complements those carried out for regular wetting [15,16]; it discusses both the thermodynamics of the transition, the exponent characterizing divergence of the film thickness and the contact angle (in an appropriately modified definition), which satisfies the modified Young's law. The thermodynamics comes from a full evaluation of the canonical partition function. The transition may also be investigated in the traditional, but possibly approximate way, from the intersection in parameter space of free-energy curves estimated for interfaces either crossing the corner through the bulk or bound to the walls. This means we assume the basic geometrical structure of interfaces and their change in the transition. Further, this estimation uses bulk angle-dependent surface tensions and wall-binding incremental free energies, which have to be calculated for the method to be useful. Clearly, there are serious approximations; fluctuations which interpolate between the two basic configurations are ignored, as are line and 'corner' tensions. It is important to note, though, that large fluctuations are not inhibited, since a proper calculation of the surface tension, for instance, allows for them. What is not considered is that the interface might 'tunnel' between the shortest path and that bound to the walls in order to decrease free energy. Further, the interface might even follow a curved path.

Given these approximations, it is reassuring that the phase diagram is indeed recaptured correctly [6,8]. Since finding an exact solution to *any wetting* problem is a lucky accident and the result of considerable labour, a different approach is desirable. Such an approach could, for instance, involve either Monte-Carlo simulations [9–11] or extending the free-energy technique as outlined above. We do both in this paper, first by finding an exact solution for wetting and surface tensions in the triangular lattice. This allows us to locate the filling phase transition line by the free-energy method and to check a conjecture for universal characteristic of the shift in boundary between wetting and filling (this is exact in the free-energy construction described above) [6]. The reader may well ask why the calculation for the filling transition in the square lattice case [8] cannot just be repeated for the triangular lattice. The problem is that *form factors* are needed in the basis defined by eigenvectors of the transfer matrix for the triangular lattice *on a half line*. Not even the eigenvectors are yet known in this case, so the rest of the argument is academic. This is why we are advocating a critical extension of other techniques available.

### 2. TRIANGULAR LATTICE SOLUTION

This is the most natural two-dimensional lattice to consider, from a packing point of view, but the spectrum of the transfer matrix had not been obtained [17] in a convenient form for the analysis of the surface properties until now. Thus, we encounter a Bogoliubov–Valatin transformation [18,19] closely analogous to that in the square lattice case [20]. As shown in Fig. 1, if we have the spectrum of the (1, 1)-direction transfer matrix (which is denoted  $T_{(1,1)}(K_1, K_2)$ ) [21], analogous results follow for the triangular lattice by bringing in the transfer operators for the horizontal  $K_3$  bonds, denoted  $V_2(K_3)$ . Thus the transfer matrix between the first and second row is

$$W(K_1, K_2) = V_2(K_3)^{1/2} T_{(1,1)}(K_1, K_2) V_2(K_3)^{1/2} \tag{1}$$

and the transfer matrix between the first and third row is

$$V = W(K_1, K_2) W^\dagger(K_2, K_1). \tag{2}$$

With the usual decomposition into odd and even Fermion number subspaces, this can be written in canonical form as

$$V_\pm = \Lambda_{\max}(\pm) \exp\left\{-\sum_{\omega} \lambda(\omega) G^\dagger(\omega) G(\omega)\right\} \tag{3}$$

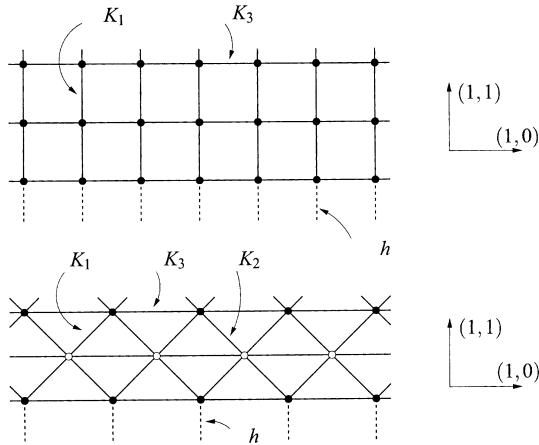


**Fig. 1.** Schematic diagram of the lattice showing the orientation of the bond labels,  $K_j$ , and the surface field,  $h$ .

with  $e^{iM\omega} = \mp 1$ ,  $\omega \in (-\pi, \pi]$  and

$$G^\dagger(\omega) = \cos \theta(\omega) F^\dagger(\omega) - i \sin \theta(\omega) F(-\omega). \tag{4}$$

The transformation angle is given by

$$e^{2i\theta(\omega)} = -e^{i\omega} \left[ \frac{(e^{i\omega} - A_\Delta)(e^{i\omega} - B_\Delta^{-1})}{(e^{i\omega} - A_\Delta^{-1})(e^{i\omega} - B_\Delta)} \right]^{1/2} \left( \frac{B_\Delta}{A_\Delta} \right)^{1/2} \tag{5}$$

with  $A_\Delta = \exp 2(K_3^* + (K_3^+)^*)$ ,  $B_\Delta = \exp 2(K_3^* - (K_3^+)^*)$ , where  $*$  denotes the usual Onsager duality and  $K_3^+$  (and mutatis mutandis  $K_j^+$ ) is given by

$$\cosh 2(K_3^+)^* = \cosh 2K_1 \cosh 2K_2 + \sinh 2K_1 \sinh 2K_2 \cosh 2K_3^*. \tag{6}$$

This is the star-triangle relationship in disguise [22]. The final result needed is

$$e^{-\lambda(\omega)} = \left( \frac{C - e^{-\gamma_\Delta(\omega)}}{C - e^{+\gamma_\Delta(\omega)}} \right) \left( \frac{\sinh 2K_1 + e^{-i\omega} \sinh 2K_2}{\sinh 2K_2 + e^{-i\omega} \sinh 2K_1} \right) \tag{7}$$

with  $C = \sinh 2K_1 \sinh 2K_2 \sinh 2K_3^+ / \sinh 2K_3$  and  $\gamma_\Delta(\omega) \geq 0$  with

$$\cosh \gamma_\Delta(\omega) = \cosh 2K_3 \cosh 2K_3^+ - \sinh 2K_3 \sinh 2K_3^+ \cos \omega. \tag{8}$$

This should be contrasted with the usual Onsager  $\gamma$  function given by

$$\cosh \gamma(\omega) = \cosh 2K_1^* \cosh 2K_3 - \sinh 2K_1^* \sinh 2K_3 \cos \omega. \tag{9}$$

Note that if  $K_1 = K_2$  then  $V = V^\dagger$  either by inspection of Fig. 1 or by direct calculation. The similarity with the elements of the Onsager hyperbolic triangle will turn out to be very useful, in particular, the al Kashi formulae for such triangles; it is not accidental but more detailed work to reveal it will be given elsewhere. Using the form of Eqs. (5), (7), and (8), we can calculate the results in a straightforward manner: firstly, the incremental free energy  $\tau_p$  for a domain wall starting at  $(1, 0)$  and ending at  $(s + 1, 0)$  in an edge along the  $(1, 0)$  direction in Fig. 1 with surface field  $h$  is given by

$$\tau_p = - \lim_{s \rightarrow \infty} \frac{1}{s} \log \left( \frac{1}{2\pi} \int_0^{2\pi} e^{is\omega} f(\omega) d\omega \right) \tag{10}$$

with

$$f(\omega) = i \tan(\delta_\Delta^*/2) \frac{e^{\gamma_\Delta(\omega)} - e^{-4K_3 w_\Delta}}{e^{\gamma_\Delta(\omega)} - w_\Delta} e^{2K_3}, \tag{11}$$

where  $\delta_\Delta^* = 2\theta(\omega) - \omega + \pi$  from Eq. (5) and  $w_\Delta$  is the wetting parameter given by

$$w_\Delta = e^{2K_3} (\cosh 2K_3^+ - \sinh 2K_3^+ \cosh 2h). \tag{12}$$

The formula for  $f(\omega)$  in the rectangular case has  $\delta_\Delta^*(\omega)$  replaced by  $\delta^*(\omega)$  and  $w_\Delta$  replaced by

$$w = e^{2K_3} \frac{\cosh 2K_1 - \cosh 2h}{\sinh 2K_1}. \tag{13}$$

The function  $\delta_\Delta^*(\omega)$  is given by (see Fig. 2)

$$\sinh 2K_3 \sinh \gamma_\Delta(\omega) \cos \delta_\Delta^*(\omega) = \cosh 2K_3 \cosh \gamma_\Delta(\omega) - \cosh 2K_3^+, \tag{14}$$

$$\frac{\sin \omega}{\sinh \gamma_\Delta(\omega)} = \frac{\sin \delta_\Delta^*(\omega)}{\sinh 2K_3^+}. \tag{15}$$

The function  $f(\omega)$  has simple poles when  $\gamma_\Delta(\omega) = \log w_\Delta$ , for which  $\omega = \pm i\nu_0, \text{ mod } 2\pi$ , where

$$\nu_0 = i\hat{\gamma}_\Delta(i \log w_\Delta) \tag{16}$$

and the function  $\hat{\gamma}_\Delta$  is given by Eq. (8) with  $K_3$  and  $K_3^+$  replaced by their dual values. Provided  $w_\Delta > 1$ , this is *nearer* the imaginary axis, then the branch points of  $\tan(\delta_\Delta^*/2)$  are  $\omega = \pm 2i(K_3^* - (K_3^+)^*), \pm 2i(K_3^* + (K_3^+)^*)$ , which characterize bulk on correlation function decay on the triangular lattice; thus, this singularity is called the wetting pole (more correctly, the partial-wetting pole). In this paper, we are interested only in the case,  $w_\Delta > 1$ .

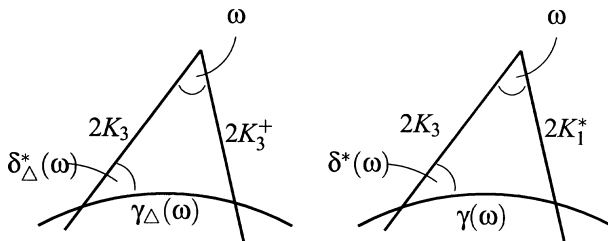


Fig. 2. Hyperbolic triangles in the Poincaré unit disc model for the triangular and rectangular lattices.

The analogy between Eqs. (11) and (12) for the square lattice case [15], which is recaptured precisely as  $K_2 \rightarrow 0$ , is striking. The length scale normal to the substrate is

$$\ell_{\perp} = \frac{1}{\lambda(iv_0)}. \quad (17)$$

Again, the  $K_2 \rightarrow 0$  limit gives the usual square lattice result  $\ell_{\perp} = 1/\hat{\gamma}(iv_0)$  with the rectangular-lattice Onsager function  $\hat{\gamma}_{\Delta}$  given by Eq. (8) with  $K_3$  replaced by  $K_1$  and  $K_3^+$  by  $K_2^*$ .

For an interface with mean direction along  $(1, 0)$  in Fig. 1, the surface tension is

$$\tau_{(1,0)} = 2(K_3^* - (K_3^+)^*) \quad (18)$$

as given by Fisher and Ferdinand [23]. To analyze filling in the  $120^\circ$  wedge, we also need  $\tau_{(1,1)}$ . For brevity, we give the result for the case  $K_j = K$ ,  $j = 1, 2, 3$ . This is

$$\tau_{(1,1)} = \lambda(0) = 4K + 2 \log \sinh 2K. \quad (19)$$

### 3. THERMODYNAMICS FOR DIFFERING GEOMETRIES

Once the thermodynamics of wetting is established, we can derive from it the filling conditions for the respective geometries by simple but, in principal, approximate thermodynamical arguments following the methods described earlier [6]. The idea is to compare the interfacial free energies of the non-filling and filling configurations at the transition temperature by using a macroscopic filling condition. For the  $60^\circ$  wedge this is particularly simple, as the interface on average always follows a lattice direction, and we derive

$$\tau_{(1,0)} = 2\tau_p \quad (20)$$

for the isotropic lattice.

For the  $120^\circ$  wedge the construction is not so simple as we must take into account the fact that the interface in the filled state will, on average, cross the lattice at an angle of  $\pi/6$ . The equivalent statement is hence

$$\tau_{(1,1)} = 2\tau_p, \quad (21)$$

where the  $(1, 0)$  and  $(1, 1)$  directions are both shown in Fig. 3 and the  $\tau$ 's have been normalized appropriately.

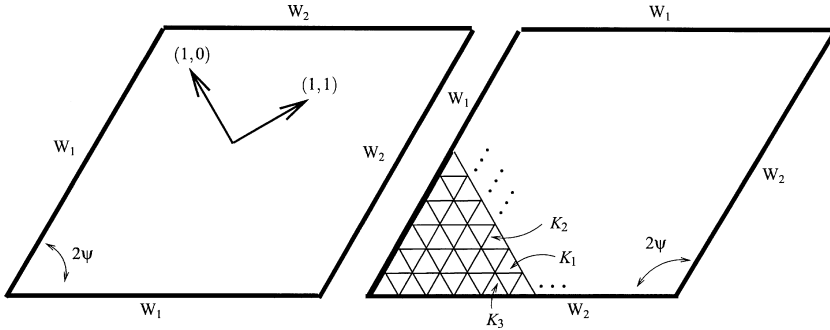


**Fig. 3.** Simulated systems (see Eq. (24)); on the left, system with 60° angle, and on the right, system with 120° angle. Part of the lattice is sketched on the right-hand side figure and axes are defined on the left.

As noted by Parry et al. [6] a useful quantity of interest, which is dependent only on the wedge opening angle  $2\psi$  (see Fig. 3) as we approach the triangular lattice bulk critical point,  $T_C^\Delta$ , is the ratio  $R(\psi)$ , defined by

$$R(\psi) = \lim_{T \rightarrow T_C^\Delta} \frac{h_F}{h_W}, \tag{22}$$

where the  $h$  fields are the critical fields in the wetting and filling cases, respectively. These fields are derived from the thermodynamic conditions, and in the square case, the ratio and its subsequent limit can be derived analytically. In this limit the lattice gains fluid isotropy and  $R(\psi)$  takes the following simple form:

$$R(\psi) = \sqrt{2} \sin \frac{\psi}{2} \tag{23}$$

for which the value of  $(2 + \sqrt{2})^{-1/2}$  was confirmed in the square case. For the triangular cases we thus predict  $R(\pi/6) = (\sqrt{3} - 1)/2$  and  $R(\pi/3) = 2^{-1/2}$ . In the triangular case the algebraic problems are more significant, and so a symbolic computer solution is more appropriate (Mathematica). We implemented and solved the quartic Eqs. (20) and (21) for  $h_F(T)$  and also the corresponding wetting equation,  $\tau = \tau_p$  for  $h_W(T)$  and took the limit of Eq. (22) resulting in 0.3660 and 0.7071 for 60° and 120° opening angles, respectively. These values agree with Eq. (23) and thus confirm the conjecture for the case being examined.

#### 4. NUMERICAL RESULTS

The filling conditions of Eqs. (20) and (21) presented in the previous section are based on a thermodynamical argument. To test if this argument is reasonable, we perform Monte–Carlo simulations to get independent estimates for the filling phase boundaries.

Defining a phase boundary for filling using conventional Monte–Carlo methods would be a daunting task because one would be forced to do a number of simulations with different surface fields and temperatures. Instead we use  $N$ -fold implementation of the Wang–Landau sampling [24] introduced by Schulz et al. [25]. In Wang–Landau sampling, a random walk in energy or any other parameter space (a point that will be exploited later) is performed to get estimates for the density of states of the parameter in question. Schulz et al. successfully combined this algorithm with the  $N$ -fold Monte–Carlo method.

Our simulated system is depicted in Fig. 3 and it has the following Hamiltonian:

$$\mathcal{H} = -\frac{K}{2} \sum_{n.n.} \sigma_i \sigma_j - h \sum_{i \in W_1} \sigma_i + h \sum_{i \in W_2} \sigma_i, \quad (24)$$

where the first sum is over nearest neighbors,  $h$  represents the strength of the surface field, and spins on the boundary belong either to set  $W_1$  or to set  $W_2$ . We assign the boundary spins depending on whether we study a  $60^\circ$  or  $120^\circ$  opening angle. Furthermore, we consider only the isotropic case, i.e., with coupling strength  $K = K_1 = K_2 = K_3$ .

After performing a simulation with the Hamiltonian above, we have an estimate for the relative density of states  $g(E(h))$  for one value of the surface field. This function can be made absolute by using the knowledge of the degeneracy of the ground state. Even though  $g(E(h))$  is indeed a desirable quantity, as it gives an opportunity to find the filling transition temperature  $T_F$  for the field  $h$ , we still face the problem of defining the transition point for different fields. To overcome this problem, instead of calculating  $g(E(h))$  for several  $h$ 's, we will consider simulating  $g(E_b, n_s)$ , where  $E_b$  is the bulk energy and  $n_s$  is the number of surface spins parallel to the boundary field minus the number of surface spins anti-parallel to the boundary field. We then calculate  $g(E(h))$  for any  $h$  using

$$g(E(h)) = \sum_{n_s} \sum_{E_b} g(E_b, n_s) \delta(E_b + n_s h - E(h)), \quad (25)$$

and, hence, quantities like the specific heat are accessible. It is perhaps worthwhile to explain why turning a one-dimensional problem ( $g(E(h))$ )



into a two-dimensional one ( $g(E_b, n_s)$ ) is useful. When a filling field  $h$  is introduced, the smooth and monotonic function  $g(E)$  decomposes into a ‘spiky’ function and the number of energy levels increases by a factor  $\sim L$ , the dimension of the system. The computing time used by the algorithm is proportional to the levels it has to visit. Even though the time for a two-dimensional distribution  $g(E_b, n_s)$  scales quadratically, it is still faster to simulate than the original one-dimensional problem; furthermore, it is indeed a smooth surface, a fact that seems to reduce errors during the simulation. To enlighten this further, we perform a post-simulation analysis for the case of a  $40 \times 40$  lattice. In this case  $g(E_b, n_s)$  for the  $120^\circ$  opening angle has altogether 357,923 levels and the set of  $g(E(h))$ ’s,  $h = 0.05, 0.10, \dots, 1.95, 2.00$  has 1,156,202 levels. Thus, simulating  $g(E_b, n_s)$  is about three times faster. Furthermore, by exploiting the obvious symmetry of  $g(E_b, n_s)$  with respect to the energy axis, an additional factor of two can be saved from the computing time. So we are transforming a difficult (in the computational sense) one-dimensional problem to an easier two-dimensional problem. This reformulation pays off if the interest is on the system’s behavior with *many* different  $h$ ’s, as is the case if we want to define filling phase boundaries.

As an indicator of the filling transition in the  $60^\circ$  (resp.  $120^\circ$ ) case we use the peak in the difference between specific heats of two systems, one with  $h = 1$  (resp. 2) field and one with the filling field  $h < 1$  (resp. 2), i.e.,  $|C(T)_{1(\text{resp.}2)} - C(T)_h|$ . In Fig. 5 one such set of peaks is depicted for a  $60^\circ$  opening angle. The parameters relevant to the simulations are collected in Table I. Even though no finite-size scaling has been done, the phase boundary extracted from simulations gives reasonably good agreement with the exact phase boundary, as can be seen in Fig. 4. Even small systems ( $30 \times 30$ ) give accurate results with large filling fields as was also the case in analogous studies with square Ising lattices with  $90^\circ$  angles [6–10]. Simulation results deviate systematically from the exact phase boundary when field  $h \rightarrow 0$ , i.e.,  $T_F \rightarrow T_C^A$ . This is a typical finite-size effect and as simulation results with  $40 \times 40$  system show, this deviation will get smaller when system size is increased. Full treatment of the finite-size effects will be considered elsewhere but for the moment we *confirm the applicability of the thermodynamical argument* for the filling condition with the numerical agreement between simulated and exact phase boundaries with large enough filling fields.

## 5. CONCLUSIONS

In summary, we have outlined the exact wetting behavior of a two-dimensional Ising ferromagnet defined on a triangular lattice. By

**Table I.** Simulation Parameters,  $\Delta s_0$ ,  $\Delta s_{\text{final}}$ , and  $\varepsilon$  are the Initial Modification Factor of the Iterated Density of States, the Final Modification Factor, and the Flatness Criterion, respectively. (The reader is referred to Ref. 25 for further details.)

$\Delta s_0$	$\Delta s_{\text{final}}$	$\varepsilon$	System size	No. of sub intervals	No. of runs
0.8685	$\leq 10^{-8}$	0.85	$30 \times 30$	5	10
0.8685	$\leq 10^{-8}$	0.85	$40 \times 40$	8	6

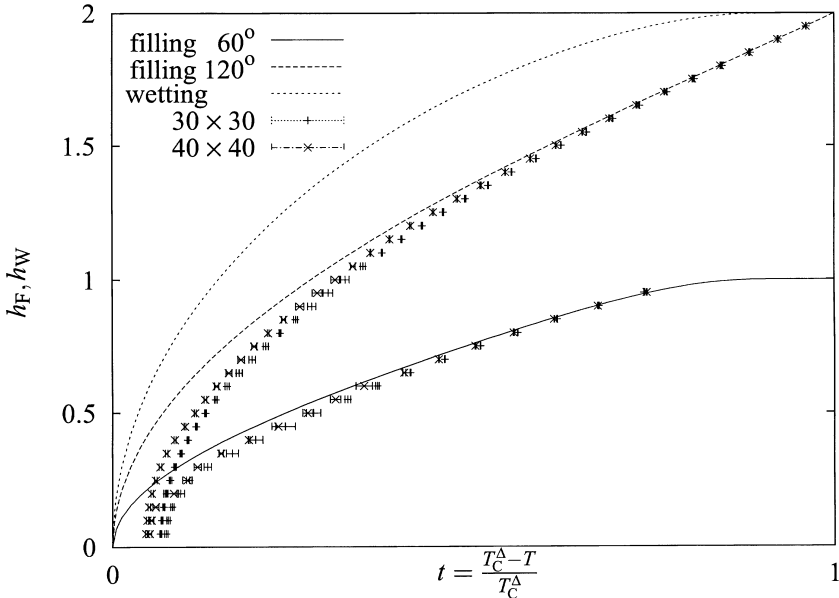


**Fig. 4.** Filling in  $60^\circ$  and  $120^\circ$  and wetting phase boundaries are plotted versus temperature from bulk critical point  $T_C^\Delta$  to  $T=0$ . Monte-Carlo data are shown for  $30 \times 30$  and  $40 \times 40$  lattices. Error bars are standard deviations calculated over the runs defined in Table I.

constructing wedges with opening angles of both  $60^\circ$  and  $120^\circ$ , we have established new results, which are almost certainly exact, for the filling behavior. These agree with our Monte-Carlo simulations, and with certain prior conjectures on the universality of a transition line shift between filling and wetting at bulk criticality. The form of our triangular lattice calculation implies that finite-size results should be available using existing methods for the surface tension and even for the wetting transition.

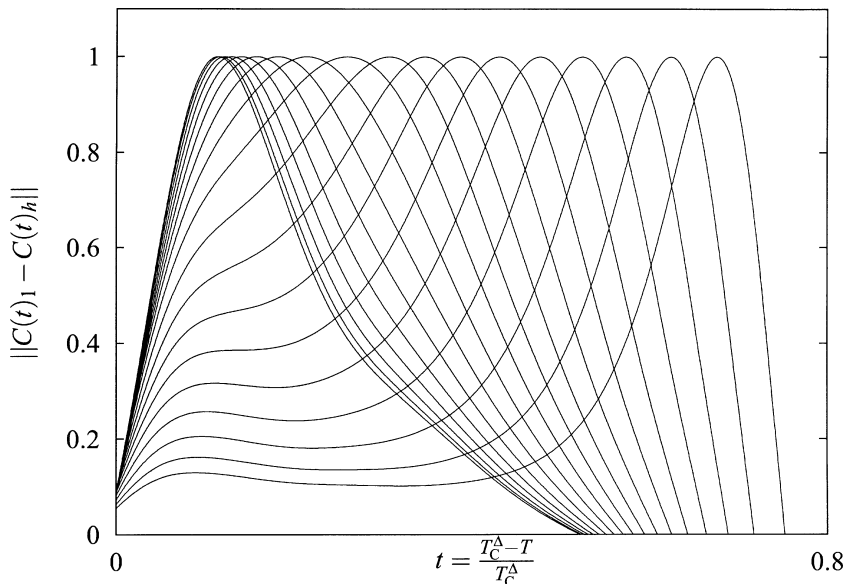


Fig. 5. Indicator of the filling transition,  $|C(t)_1 - C(t)_h|$ , is shown for fields  $h = 0.05, 0.10, \dots, 0.95$  for the  $60^\circ$  opening angle. Curves are normalized.

## ACKNOWLEDGMENTS

DBA and AJW would like to acknowledge financial support from the EPSRC under Grant No. GR/M04426 and the Royal Commission for the Exhibition of 1851, respectively. VM was partially supported by the Academy of Finland, Research Centre for Computational Science and Engineering, Project No. 44897 (Finnish Centre of Excellence Programme 2000–2005), Wihuri Foundation, Finnish Cultural Foundation and Tekniikan edistämissäätiö. Computing time made available by collaboration of Laboratory of Computational Engineering (Helsinki University of Technology) and Wolfson College (Oxford) is greatly appreciated.

## REFERENCES

1. S. Dietrich, in *Proc. NATO-ASI—New Approaches to Old and New Problems in Liquid State Theory*, C. Caccamo, J. P. Hansen, and G. Stella, eds. (1999), pp. 197–244.
2. K. Rejmer, S. Dietrich, and M. Napiórkowski, *Phys. Rev. E* **60**:4027 (1999).
3. A. O. Parry, C. Rascón, and A. J. Wood, *Phys. Rev. Lett.* **83**:5535 (1999).
4. A. O. Parry, C. Rascón, and A. J. Wood, *Phys. Rev. Lett.* **85**:345 (2000).
5. A. O. Parry, A. J. Wood, and C. Rascón, *J. Phys. Cond. Matt.* **13**:4591 (2001).
6. A. O. Parry, A. J. Wood, E. Carlon, and A. Drzewiński, *Phys. Rev. Lett.* **87**:196103 (2001).

7. D. B. Abraham, A. O. Parry, and A. J. Wood, *Euro. Phys. Lett.* **60**:106 (2002).
8. D. B. Abraham and A. Maciolek, *Phys. Rev. Lett.* **89**:286101 (2002).
9. A. Milchev, M. Müller, K. Binder, and D. P. Landau, *Phys. Rev. Lett.* **90**:136101 (2003).
10. E. V. Albano, A. de Virgiliis, M. Müller, and K. Binder, *J. Phys. Condens. Matter* **15**:333 (2003).
11. K. Binder, D. P. Landau, and M. Müller, *J. Stat. Phys.* **110**:1411 (2003).
12. M. Trau, N. Yao, E. Kim, Y. Xia, G. M. Whitesides, and I. A. Aksay, *Nature* (London) **390**:674 (1997).
13. Y. N. Xia and G. M. Whitesides, *Angew. Chem. Int. Ed. Engl.* **37**:551 (1998).
14. D. J. Durian and C. Franck, *Phys. Rev. Lett.* **59**:555 (1987).
15. D. B. Abraham, *Phys. Rev. Lett.* **44**:1165 (1980).
16. D. B. Abraham and L. F. Ko, *Phys. Rev. Lett.* **63**:275 (1989).
17. R. M. F. Houtappel, *Physica* **16**:425 (1950).
18. N. N. Bogoliubov, *Nuovo Cimento* **7**:794 (1958).
19. J. G. Valatin, *Phys. Rev.* **122**:1012 (1961).
20. T. D. Schulz, D. C. Mattis, and E. H. Lieb, *Rev. Mod. Phys.* **36**:856 (1964).
21. D. B. Abraham and B. Davies, to be published.
22. R. J. Baxter, *Exactly Solvable Models in Statistical Mechanics* (Academic Press, New York, 1982).
23. M. E. Fisher and A. E. Ferdinand, *Phys. Rev. Lett.* **19**:169 (1967).
24. F. Wang and D. P. Landau, *Phys. Rev. Lett.* **86**:2050 (2001).
25. B. J. Schulz, K. Binder, and M. Müller, *Int. J. Mod. Phys. C* **13**:477 (2002).